ARTICLE NO. 78-819

Optimum Design of Wind Tunnel Contractions

M. N. Mikhail*
Faculty of Engineering, Cairo University, Egypt

A method for the design of low-speed wind tunnel contractions is presented. An optimum contraction is considered to be the shortest one that satisfies flow quality requirements in the test section; i.e., avoids any boundary-layer separation and supplies flow to the test section with a specified degree of uniformity. It is shown that by optimizing duct wall curvature distribution, it is possible to reduce contraction length to about one-half of that presently used in practice for a given test section flow quality. For example, a contraction with an area ratio of eight for a large wind tunnel can be as short as one inlet radius. The present method closely relates the shape and length of the contraction to the degree of flow quality required in the test section, to the contraction ratio, to the inlet flow Reynolds number, and to the viscous flow conditions in the settling chamber upstream of the contraction inlet. Presented are data to guide the design of a contraction of any combination of these parameters. The results of the study indicate that the avoidance of turbulent boundary-layer separation near the exit need not be a design driver; rather, the possibility of boundary-layer relaminarization near the exit needs attention.

Introduction

WIND tunnels usually have a contracting duct fitted upstream of their working section to insure uniform, steady, low-turbulence flow. For wind tunnels in general, the test section size, range of airspeeds, and required flow quality are defined by the kind of tests specified for a particular tunnel. It is clear that the above aerodynamic requirements can be achieved by a variety of configurations; thus, optimization of the geometric parameters of the wind-tunnel circuit to achieve the best economy is necessary. One of the most important parameters for such optimization is the area ratio of the contracting duct (CR).

For closed-circuit wind tunnels, increasing the contraction ratio, in general, increases the tunnel physical dimensions. From an economic point of view this has two opposite effects. On the one hand, this means higher shell construction costs; on the other hand, a larger circuit leads to more efficient diffusion and fewer aerodynamic losses due to the lower flow speeds. In addition, fewer flow conditioning devices are required in the settling chamber with a higher contraction ratio. The lower losses result in smaller drive power and hence less power consumption during tunnel running. Thus, an optimum contraction ratio from an economic viewpoint can generally be defined.

Once the area ratio for the contraction is chosen, the design problem is reduced to the definition of the shortest wall shape that satisfies the flow requirements. A short contraction is advantageous from a cost viewpoint and facilitates the design of more efficient circuit elements such as diffusers in situations where only limited space is available. An elementary argument can show that, because of the wall curvature, regions of adverse pressure gradient will appear near the wall at both inlet and outlet of a finite length contraction (Fig. 1). If the adverse pressure gradient is allowed to become severe enough to cause boundary-layer separation, this could degrade the flow quality and steadiness in the test section.

Due to the absence of a satisfactory method of contraction design, existing contractions have largely been designed either by eye or by applying necessary modifications to one of the available methods. In either case, the final design depends on the ingenuity and experience of the designer, and the design process is more art than science. The purpose of the present work is to systemize the contraction design process and relate the design method to the requirements.

In reviewing the available methods of contraction design, one faces the surprising fact that, until recently, most of the effort[1-7] has been directed toward the mathematical solution of the incompressible, inviscid flow equations with little regard to the physical conditions of a real wind tunnel contraction. Just recently, however, four independent pieces of work, addressing the complete problem with the aid of large-scale computing machinery, have appeared.[8-11] This paper is based on the work of Ref. 11.

Chmielewski[8] specified a streamwise acceleration distribution. He used two parameters to choose the shortest contraction that avoided boundary-layer separation at the contraction inlet. This study carried contraction design methodology one step beyond that of previous investigations by including quantitative consideration of boundary-layer behavior.

Morel[9] was the first to publish a study that explicitly considered flow uniformity at the contraction exit as a deciding factor in contraction design. The contraction contours were formed of two cubic arcs joined smoothly together at an inflection point. Design charts are presented to define the required contraction length and position of the inflection

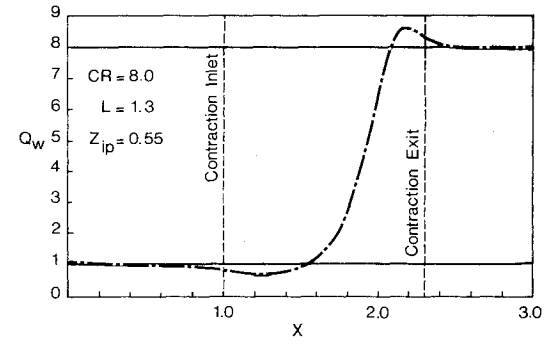

Fig. 1 Typical velocity distribution along the contraction wall.

Presented as Paper 78-819 at the AIAA 10th Aerodynamics Testing Conference, San Diego, Calif., April 19-21, 1978; submitted May 5, 1978, revision received Dec. 11, 1978.

Index categories: Nozzle and Channel Flow; Subsonic Flow; Analytical and Numerical Methods.

*Lecturer. Member AIAA.

point in terms of the allowable pressure coefficients at inlet and exit, determined by separation and flow uniformity requirements, respectively. Reference 9 was also the first study to point out the fact that for fixed requirements the necessary contraction length decreases as the contraction ratio increases (for CR > 4).

Borger[10] used a polynomial of the fifth degree to describe the contraction contour. The coefficients of the polynomial are chosen to produce the minimum length contraction that avoids boundary-layer separation at both inlet and exit and provides uniform flow at the contraction exit. Contractions produced by this method are characterized by almost a circular arc contour in the inlet region and by a short exit region. A slight expansion near the contraction exit is recommended to improve the uniformity of the flow to the test section. The results of Borger's study concerning the contraction length variation with contraction ratio are essentially in agreement with those of Ref. 9 and the present results.

The present work, as in Ref. 11, is based on the hypothesis that by optimizing the duct curvature distribution, one can keep both the pressure gradient and flow nonuniformity within tolerable ranges while using short contraction. The specific reasons for following that approach are: 1) The duct-wall curvature is directly responsible for the adverse pressure gradient developing near the inlet and exit of the contraction. 2) The wall curvature, near the exit, in particular, is responsible for the nonuniformity of the flow to the test section. 3) Close examination of the governing equations and the necessary boundary conditions (as will be discussed later) show that the flow is sensitive only to the duct radius, slope, and curvature; hence, the judgment that optimizing the duct R'' distribution would be the most suitable. 4) By making R'' distribution as general as practicality permits, we can almost cover all feasible contraction shapes. Actually, the six parameters family of contours used in here comes very close to achieving that goal (discussed further in the next section). The approach taken here has been successful in producing short contractions, as will be evident from the following sections.

Analysis

Geometrical Model

An axisymmetrical model for the settling chamber, contraction, and test section combination, as shown in Fig. 2, is used.

The distribution chosen for the second derivatives of the contraction coordinate takes the form (nomenclature, see Fig. 3):

For the inlet section:

$$R'' = -A_1(1+B_iZ_1)[\sin(\pi Z_1)]^{N_i} \quad \text{for } 0<Z_1<1$$

and for the exit section:

$$R'' = A_2(1+B_eZ_2)[\sin(\pi Z_2)]^{N_e} \quad \text{for } 0<Z_2<1$$

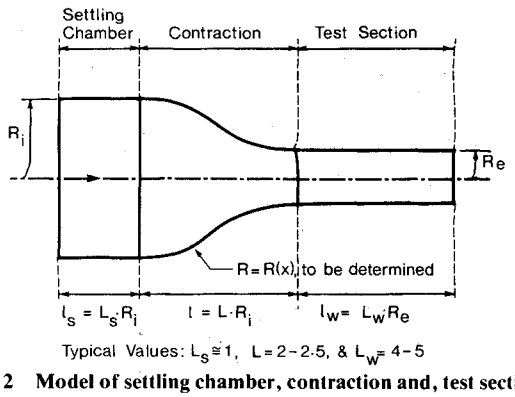

Fig. 2 Model of settling chamber, contraction and, test section.

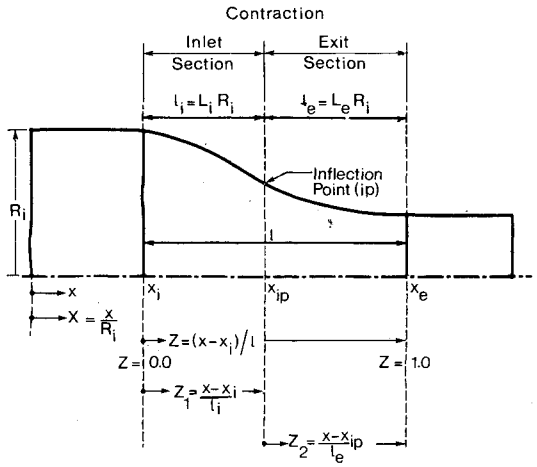

Fig. 3 Illustration of the nomenclature.

A_1 and A_2 are factors to be defined to give the required contraction ratio and to satisfy zero wall slope at inlet and exit. The B's control the position of the local peaks of the distribution. For $B=0$, the peak is at the middle. Negative values for B move the peak upstream, while positive values move it downstream. The N's control the pointness ($N>1$), or squareness ($N<1$) of the distribution shape.

For a given contraction ratio and inlet radius R_i, the parameters to be chosen through the optimization process are inlet section length L_i, exit section length L_e, and the parameters B_i, N_i, B_e, and N_e.

The above suggested method of generating contraction shapes is quite general and does produce shapes very close to previously studied contraction geometries as special cases. The following are some examples:

1) With $N_i=3.0$, $B_i=0.5$, $N_e=0.1$, and $B_e=0.0$, the contraction shape will be close to that of Ref. 8.

2) With $N_i=1.0$, $B_i=1.5$, $N_e=0.1$, and $B_e=-1.0$, the contraction shape will be close to that of Ref. 9.

3) With $N_i=0.01$, $B_i=0.0$, $N_e=1.0$, and $B_e=0.0$, the contraction shape will be close to that of Ref. 10.

Inviscid Flow Calculations

The inviscid incompressible flow in an axisymmetric duct is governed by the Stokes-Beltrami equation:

$$\psi_{xx} - \frac{1}{r}\psi_r + \psi_{rr} = 0$$

where ψ is Stokes stream function. This equation, with the appropriate boundary conditions, is solved for the flow inside the duct defined in Fig. 2. A coordinate transformation is utilized, such that the calculation domain is rectangular with fixed boundaries. The transformation takes the form:

$$\eta - (R/R_w) = [R/F(X)] \quad \text{and} \quad \xi = X$$

The governing equation then becomes

$$\psi_{\xi\xi} = C\psi_\eta + D\psi_{\eta\eta} + E\psi_{\eta\xi}$$

where C, D, and E are functions of R, R', and R''.[11] Through the preceding transformation, the duct shape parameters appear in the governing equation rather than in the boundary conditions. In addition to the simplicity gained in the numerical solution, examining the terms of the transformed equation gives an insight into the geometrical parameters affecting the flow. It is clear that the duct coordinate and its derivatives up to the second derivative (but not higher) has an effect on the flow inside the duct.

The method of lines[12] is used for the solution of the inviscid flow. A computer program has been developed and tested for accuracy against a closed-form solution of one of Thwaites' contractions.[4]

Boundary-Layer Flow

A turbulent boundary layer is assumed to originate at the last flow-conditioning screen in the settling chamber. Stratford's criterion for turbulent separation[13] is used as a fast and effective method of judging the effect of different design parameters on possible boundary-layer separation. After bracketing the different parameters in a relatively narrow range, detailed boundary-layer calculations were made for the final selection of optimum values. The boundary-layer calculations were made using a computer program based on the "lag-entrainment" method of Green et al.[14] The version of the boundary-layer calculations used considers the effects of the wall curvature on the boundary-layer flow. In the present analysis, the boundary layer is assumed to start in the settling chamber one local radius upstream of the contraction inlet. The effect of varying that distance is then examined and presented later.

The flow acceleration near the walls in the middle part of a short contraction is very high. In comparatively low Reynolds number situations, this can cause changes in the turbulent structure of the boundary layers and relaminarization has been correlated with one parameter[15,16]:

$$K = \frac{\nu}{U^2}\frac{dU}{dx}$$

(or with a combination of K and local skin friction coefficient C_f). However, as a result of the fact that relaminarization is a gradual and slow process, it is not really possible to associate its occurrence with a specific local value of K. Nevertheless, experiments[16] have shown that when K exceeds a value of about 2×10^{-6}, relaminarization effects will, in general, become significant. In the present study, this value for K is taken as an indication of a possible change in the boundary-layer structure and, hence, presents a limit on the application of Stratford's turbulent separation criterion at the contraction exit. It was not judged to be valid to use Stratford's criterion for laminar boundary-layer separation[17] downstream of such conditions. (For the present purpose, it was decided that such situations should be avoided.)

The physical dimensions used here for the viscous flow calculations are chosen to be representative of typical data for large modern wind tunnels; the contraction ratio is 8 and the inlet radius is 40 ft. The conditions in the settling chamber are a pressure of one bar and an air temperature of 100°F. The Reynolds number based on inlet diameter is then 1.3×10^7. The effect of variation of these data on the optimum design of the contraction is investigated and reported later in the paper.

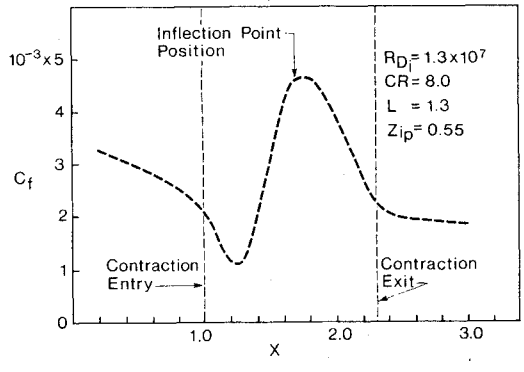

Fig. 4 Distribution of local skin friction coefficient through a contraction.

Results and Discussions

Figures 4 and 5 show the boundary-layer behavior as calculated using the "lag-entrainment" method and the velocity distribution of Fig. 1. The rapid thickening and approach to boundary-layer separation in the entry section of the contraction is evident.

Extensive investigations[11] indicate that although boundary-layer separation could occur at the contraction inlet, the exit region is safe from boundary-layer separation as long as the boundary layer stays turbulent. Consistently, independent of the shape and no matter how short the exit section of the contraction is made, the boundary-layer relaminarization criterion is reached before any separation at exit is indicated.

Effect of the Geometrical Parameters

Inlet Section Parameters

The effect of N_i on the pressure coefficient at the contraction inlet is shown in Fig. 6. (C_{P_i} is defined in the Appendix.) Decreasing N_i, i.e., increasing the squareness of the inlet R'' distribution, leads to a lower maximum C_{P_i} but little change in pressure gradient. The net effect, however, is beneficial from an inlet separation point of view. Variation of N_i resulted in little change in flow at the exit section of the contraction.

The effect of B_i on the pressure coefficient at the contraction inlet is shown in Fig. 7. This shows that it is beneficial to move the peak of the inlet section R'' distribution downstream assigning positive values for B_i, since this results in reducing both the magnitude and gradient of the pressure coefficient at inlet C_{P_i}. Again, the effect of B_i on the flow characteristics in the exit section is minimal.

The effect of L_i, the nondimensional inlet length, on the pressure coefficient at the inlet is shown in Fig. 8. It is clear

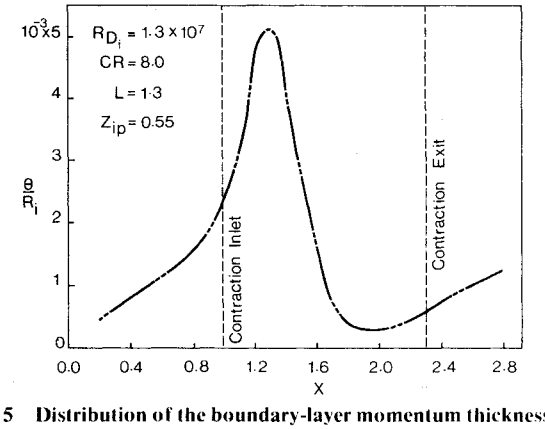

Fig. 5 Distribution of the boundary-layer momentum thickness θ.

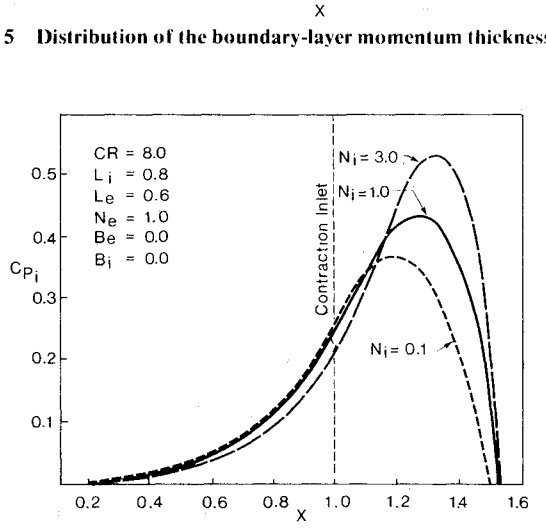

Fig. 6 Effect of N_i on the pressure coefficient distribution at contraction inlet.

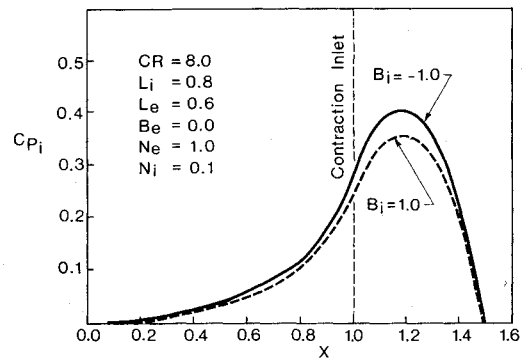

Fig. 7 Effect of B_i on the pressure coefficient distribution at contraction inlet.

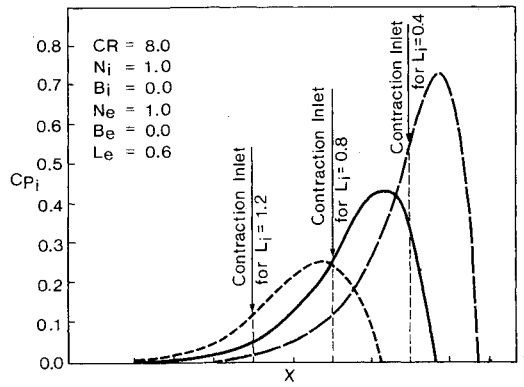

Fig. 8 Effect of the contraction inlet section length L_i on the pressure coefficient distribution at inlet.

that L_i has a decisive effect on the flow in the inlet section, since it directly controls both the magnitude and gradient of the pressure. Also, it has an effect on both the pressure coefficient at exit and the flow uniformity to the test section, but this is less important than the local effects (at inlet).

Figure 8 shows that the "affected" upstream length increases as the contraction length decreases. In order to avoid adversely affecting the flow uniformity, the upstream influence should not extend up to the last screen. This important requirement has been observed throughout the study.

Exit Section Parameters

The effect of the parameters N_e, B_e, and L_e on the local (exit) flow characteristics is qualitatively similar to the corresponding effect of the inlet section parameters. The upstream effects of the exit section geometry, although less pronounced than the local effects, cannot be completely ignored. For example, keeping the inlet section shape and length unchanged, boundary-layer separation at inlet can be induced by sufficiently shortening exit section length and/or changing its shape. Figure 9 shows this effect; namely, that separation at the contraction inlet can occur if the contraction exit section is too short even if the inlet section is sufficiently long. (MS is defined in the Appendix.)

The effect of the exit section length on the exit plane flow uniformity is shown in Fig. 10. The flow uniformity is defined as the velocity deviation from its nominal value expressed as a percentage of the nominal value.

Optimum Contraction

The choice of the optimum values for all six parameters took a number of iterations. Presented here are the results of the "last" iteration, wherein one parameter is varied with the others set at their "finally" chosen values.

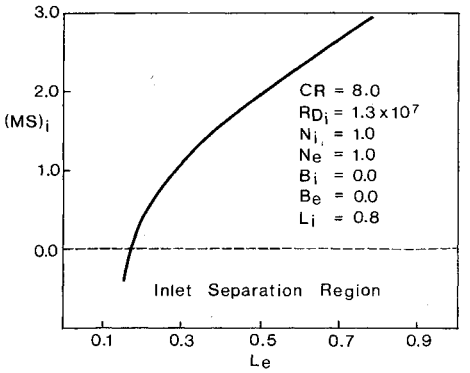

Fig. 9 Effect of exit section length on inlet boundary-layer margin of safety.

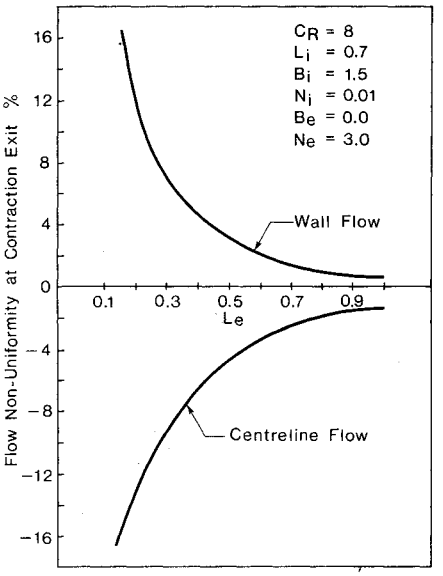

Fig. 10 Effect of exit segment length on flow nonuniformity.

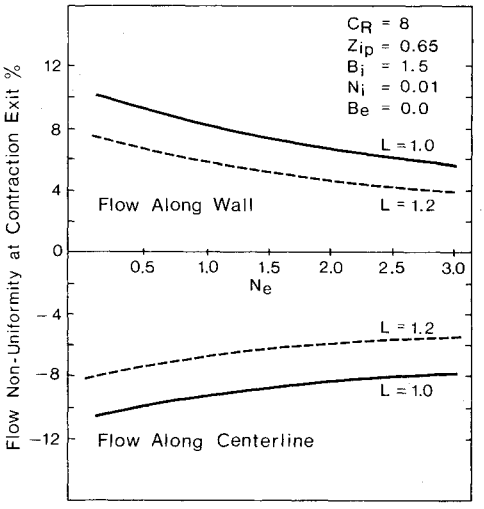

Fig. 11 Effect of N_e on flow nonuniformity.

Optimum Shape Parameters

The inlet parameters N_i and B_i were chosen to maximize the boundary-layer separation margin of safety (see the Appendix for definition). As discussed before and shown in Table 1, it is better to use small N_i and large positive B_i. No appreciable change in the contraction shape, or consequent influence on inlet separation, occurred for N_i less than 0.01 or B_i larger than 1.5 and, therefore, these values are selected.

Table 1 Effect of inlet shape parameters N_i and B_i on flow at contraction inlet and exit[a]

	$B_i = 1.5$			$N_i = 0.01$			
N_i	$(MS)_i$	$(MS)_e$	$(Q)_{max}/U_0$	B_i	$(MS)_i$	$(MS)_e$	Q_{max}/U_0
3.0	−5.7	8.4	1.14	−1.00	−1.4	8.6	1.125
1.0	−1.6	8.3	1.14	−0.50	−0.5	8.4	1.131
0.2	0.5	8.3	1.14	0.0	−0.0	8.4	1.134
0.01	0.7	8.3	1.14	0.50	0.3	8.4	1.136
				1.00	0.5	8.4	1.137
				1.50	0.7	8.3	1.138

[a] $CR = 8.0$, $R_{D_i} = 1.3 \times 10^7$, $L_i = 0.65$, $L_e = 0.45$, $B_e = 0.0$, $N_e = 3.0$.

Table 2 Effect of B_e on flow uniformity at contraction exit plane[a]

	Flow nonuniformity, %	
B_e	Along wall	Along centerline
−1.0	2.37	−6.45
−0.5	2.70	−7.17
0.0	3.00	−7.70
0.5	3.16	−7.74

[a] $CR = 8.0$, $L_i = 0.65$, $L_e = 0.35$, $B_i = 1.5$, $N_i = 0.01$, $N_e = 3.0$.

The exit section shape parameters are selected essentially on the basis of the flow uniformity at the contraction exit. Figure 11 shows that the flow uniformity at the contraction exit plane improves gradually for higher values of N_e (i.e., as the R'' distribution becomes peaky). An $N_e = 3$ is chosen since no appreciable improvement is gained by using a higher value. The stronger effect of contraction length is also shown on Fig. 11.

Table 2 shows the effect of B_e on the contraction exit plane flow uniformity. As expected, negative values of B_e result in improved flow uniformity, since the peak of the R'' distribution is moved upstream. The negative values of B_e adversely affect the inlet flow; i.e., reduce the boundary-layer separation margin of safety as shown in Fig. 12. For that reason, it was decided as a compromise to keep the peak of the R'' distribution at the middle of the section by selecting $B_e = 0.0$.

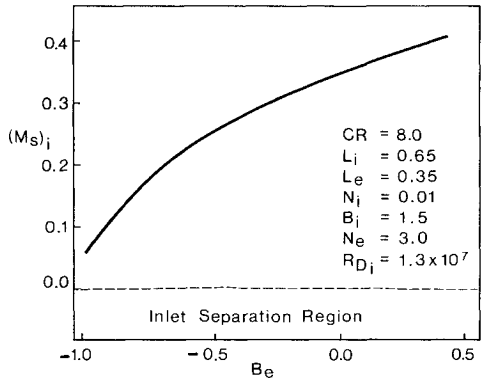

Fig. 12 Effect of B_e on inlet boundary-layer margin of safety.

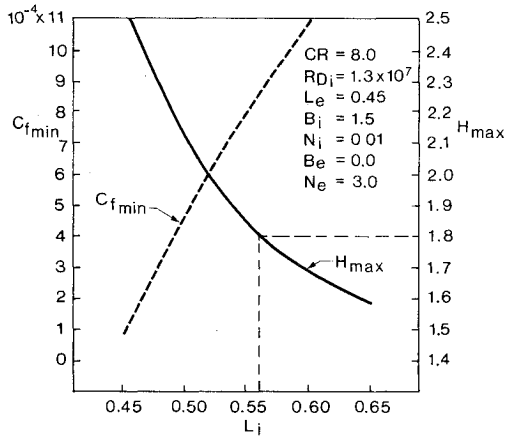

Fig. 13 Effect of inlet segment length on minimum local skin friction and on maximum shape factor in the inlet region.

Contraction Length

The choice of inlet length is essentially based on avoiding boundary-layer separation in the inlet region. The results of Fig. 13, which are based on boundary-layer lag-entrainment calculations, show that if a value of the boundary-layer shape factor H of 1.8 is adopted to indicate possible separation, as is often used with integral methods of calculation, the inlet segment length can be as short as $L_i = 0.57$. An inlet length of 0.6 has been chosen for the specified conditions.

The length of the exit section is determined on the basis of achieving 0.25% flow uniformity at a point on the test section centerline one local radius downstream from the contraction exit. It was found that the decay of the deficiency of the velocity along the centerline is slower than the decay of the velocity excess along the wall. To achieve this required

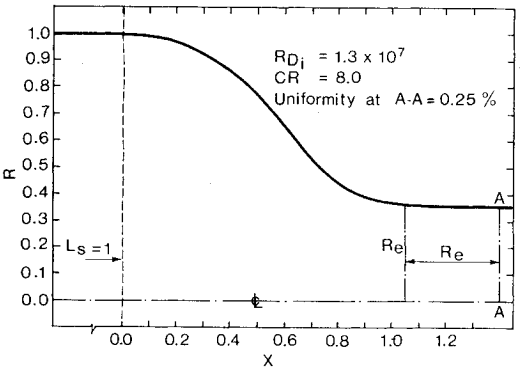

Fig. 14 Contour of the optimum contraction.

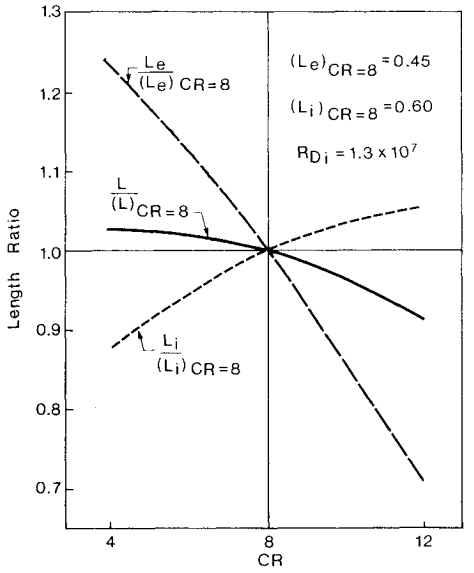

Fig. 15 The contraction optimum length as a function of the contraction ratio.

Table 3 Required contraction exit length for 0.25% flow uniformity[a]

Flow settling length/ Test section radius	Required L_e
1.5	0.15
1.0	0.45
0.5	1.00

[a] $L_i = 0.7$, $B_i = 1.5$, $N_i = 0.01$, $CR = 8.0$, $B_e = 0.0$, $N_e = 3.0$.

uniformity at the centerline, an exit length of $L_e = 0.45$ is required.

The contraction designed here would have a total length of 1.05 times its inlet radius for the assumed "standard" conditions. This is a big reduction in length compared to the typical values of 2-2.5 inlet radii presently used for a similar kind of requirement. Figure 14 shows the shape of the contraction so designed.

Variation of Basic Aerodynamic Parameters

The contraction design just presented is for a specific (but typical) set of conditions and requirements. The effect of variation of these data on the optimum design is discussed here. In all cases, the shape parameters (B's and N's) are fixed at their previously chosen values and, consequently, the general shape of the R'' distribution is maintained. This is the case, since their choice is based on the trend of their effects rather than to achieve specific requirements. The lengths of both the contraction inlet and exit sections have to be defined for different design parameters. The effect of the important aerodynamic parameters on the required contraction length is presented here in the form of the effect of variation of one parameter at a time from the standard conditions.

Flow Uniformity Requirements

The required exit section length is very sensitive to the method of specifying test section flow uniformity. Keeping the magnitude requirement of 0.25% uniformity, Table 3 shows the required contraction exit section length L_e as a function of the location at which the uniformity requirement is imposed. It is clear that the test section "settling length" allowed is an important factor in deciding on the contraction design, specifically in determining the exit section length.

Contraction Ratio

In order to avoid boundary-layer separation at inlet, the inlet length L_i should be increased with the contraction ratio according to a relation derived in Ref. 11.

$$L_i \propto \left[1 - \frac{1}{(CR)^{1/2}}\right]^{1/2}$$

The preceding relation has been confirmed by numerical examples and is presented in Fig. 15. For the same test section flow quality, the variation of the exit section length is also as shown in Fig. 15. As the contraction ratio increases, the required relative length for the exit section decreases. The variation of the total contraction length is not large, due to the offsetting influences as shown in Fig. 15. Note that the inflection point moves downstream as the contraction ratio increases.

Boundary-Layer Origin

In the analysis just presented, the turbulent boundary layer was assumed to start from an origin in the settling chamber at a distance of one local radius from the contraction inlet ($L_s = 1$). Consideration of Stratford's criterion for turbulent separation[11] indicates that the required length for the contraction inlet section L_i varies with L_s according to

$$L_i \propto (L_s)^{0.22}$$

This relation has been checked numerically and found to be applicable.[11] The exit length essentially remains unchanged.

Reynolds Number Scale

Again, consideration of Stratford's criterion for turbulent separation showed that to avoid boundary-layer separation, the contraction inlet section length varies as[11]:

$$L_i \propto (R_{D_i})^{-0.06}$$

The exit section length remains essentially unchanged. The preceding relation has also been examined numerically and found to be valid.[11] However, a problem is encountered at low Reynolds number because, in general, the criterion for possible boundary-layer relaminarization is exceeded. To avoid boundary-layer relaminarization at low Reynolds number, a longer contraction is perhaps necessary. For example, at a Reynolds number of $R_{D_i} = 1.3 \times 10^6$, the required length according to the above discussions should be $L = 1.26$. A check on the flow acceleration parameter K showed that it exceeded its previously chosen critical value of $K = 2 \times 10^{-6}$ over a considerable length of the contraction wall. To avoid that situation, the contraction length would have to be increased to $L = 1.8$. Presumably, however, appropriately placed local surface roughness could eliminate this low Reynolds number relaminarization problem.

Conclusions

1) The present study relates contraction design and the necessary contraction length to the required test section flow steadiness and uniformity.

2) Unless the contraction is carefully designed, the danger of boundary-layer separation exists at the inlet. It is found that due to the particular flow conditions in a contraction—namely, the large overall acceleration—a turbulent boundary-layer flow is able to overcome the adverse pressure gradient at outlet without danger of separation.

3) An optimum shape for the contraction curvature R'' distribution has been defined which permits the design of contractions half as long as those currently employed.

4) The required flow uniformity in the test section (both in magnitude and position) is an important factor in dictating contraction length.

5) The required contraction length for fixed requirements decreases as the contraction ratio increases in the range $4 < CR < 12$. The variation in the total length is not large, though the shape of the contraction varies significantly since the inflection point moves downstream for higher contraction ratios.

6) The contraction, as expected, can be made shorter for higher Reynolds number application. For low Reynolds number applications, a problem might be encountered regarding boundary-layer relaminarization.

7) Shorter contractions can be used whenever a thinner boundary layer exists at the contraction inlet.

8) Using the optimum shape of a contraction designed for the reference conditions together with the effect of variations in the contraction ratio and the aerodynamic parameters as indicated, a contraction for any required contraction ratio and flow conditions can be designed.

Appendix—Definitions

A. Inlet Pressure Coefficient

The inlet pressure coefficient is defined as:

$$C_{p_i} = 1 - (q_w/u_i)^2$$

where u_i is the uniform inlet velocity and q_w is the flow speed at the wall.

B. Margin of Safety (MS) for Boundary-Layer Separation

According to Stratford's criterion for turbulent separation[13] at the point of separation:

$$C_p\left(s\frac{dC_p}{ds}\right)^{1/2} = C(10^{-6}R_s)^{0.1} \text{ for } C_p < \frac{4}{7} \qquad \text{(A1)}$$

where C is an empirical constant and s is the distance from the boundary layer effective origin. We can define a margin of safety (MS) for boundary-layer separation as:

$$\text{MS} = \text{minimum (LH-RH)}$$

where LH and RH are the left-hand and right-hand side of Eq. (A1), respectively. Boundary-layer separation occurs if MS is equal to or less than zero.

Acknowledgment

The author wishes to acknowledge the contributions of W. J. Rainbird, who suggested the problem, during the course of the study. Also, the help of D. J. Jones, Head of the Computation Group, National Aeronautical Establishment, National Research Council of Canada, is greatly appreciated.

References

[1] Tsien, H., "On the Design of the Contraction Cone for a Wind Tunnel," *Journal of the Aeronautical Sciences*, Vol. 10, Feb. 1943, pp. 68-70.

[2] Szczeniowski, B., "Contraction Cone for a Wind Tunnel," *The Journal of the Aeronautical Sciences*, Vol. 10, Oct. 1943, pp. 311-312.

[3] Batchelor, G. K. and Shaw, F. S., "A Consideration of the Design of Wind Tunnel Contractions," Rept. ACA-4, March 1944.

[4] Thwaites, B., "On the Design of Contractions for Wind Tunnels," Aeronautical Research Council, R&M 2278, March 1946.

[5] Whitehead, L. G., Wu, L. Y., and Waters, M.H.L., "Contracting Duct of Finite Length," *The Aeronautical Quarterly*, Vol. II, Feb. 1951, pp. 254-271.

[6] Cohen, M. J. and Ritchie, N.J.B., "Low Speed Three-Dimensional Contraction Design," *Journal of Royal Aeronautical Society*, Vol. 66, April 1962, pp. 231-236.

[7] Bossel, H. H., "Computation of Axisymmetric Contractions," *AIAA Journal*, Vol. 7, Oct. 1969, pp. 2017-2020.

[8] Chmielewski, G. E., "Boundary Layer Considerations in the Design of Aerodynamic Contractions," *Journal of Aircraft*, Vol. 11, Aug. 1974, pp. 435-438.

[9] Morel, T., "Comprehensive Design of Axisymmetric Wind Tunnel Contractions," *Journal of Fluids Engineering, ASME Transactions*, June 1975, pp. 225-233.

[10] Borger, G. G., "The Optimization of Wind Tunnel Contractions for the Subsonic Range," NASA TTF-16899, March 1976.

[11] Mikhail, M. N., "Optimum Design of Internal Flow Passages with Specific Reference to Wind Tunnel Contractions," Ph.D. Thesis, Carleton University, Ottawa, Canada, Oct. 1976.

[12] Jones, D. J., South, J. C., and Klunker, E. B., "On the Numerical Solution of Elliptic Partial Differential Equations by the Method of Lines," *Journal of Computational Physics*, Vol. 9, June 1972, pp. 496-527.

[13] Stratford, B. S., "The Prediction of Separation of the Turbulent Boundary Layer," *Journal of Fluid Mechanics*, Vol. 5, Jan. 1959, pp. 1-16.

[14] Green, J. E., Weeks, D. J., and Brooman, J.W.F., "Prediction of Turbulent Boundary Layers and Wakes in Compressible Flow by a Lag-Entrainment Method," R.A.E. TR-72231, 1973.

[15] Launder, B. E., "Laminarization of the Turbulent Boundary Layer in a Severe Acceleration," *Journal of Applied Mechanics*, Vol. 31, Dec. 1964, p. 707.

[16] Back, L. H., Cuffel, R. F., and Massier, P. F., "Laminarization of a Turbulent Boundary Layer in Nozzle Flow," *AIAA Journal*, Vol. 7, April 1969, p. 730.

[17] Stratford, B. S., "Flow in the Laminar Boundary Layer Near Separation," Aeronautical Research Council, R&M 3002, Nov. 1954.